AGU PUBLICATIONS

Geophysical Research Letters

RESEARCH LETTER
10.1002/2016GL072277

Key Points:
- Under a low-pressure condition, the methane hydrate is decomposed through a rapid sublimation of water from the surface of hydrate crystals
- The hydrated salt of NaCl · $2H_2O$ undergoes a phase transition into a crystal growth of crystalline NaCl via the migration of salt ions
- The methane hydrate is fully decomposed in brine solutions at temperatures above 252 K, the eutectic point of NaCl · $2H_2O$

Supporting Information:
- Supporting Information S1

Correspondence to:
J.-H. Yoon,
jhyoon@kmou.ac.kr

Citation:
Shin, D., et al. (2017), Temperature- and pressure-dependent structural transformation of methane hydrates in salt environments, *Geophys. Res. Lett.*, *44*, 2129–2137, doi:10.1002/2016GL072277.

Received 8 DEC 2016
Accepted 16 FEB 2017
Accepted article online 18 FEB 2017
Published online 4 MAR 2017

Temperature- and pressure-dependent structural transformation of methane hydrates in salt environments

Donghoon Shin[1], Minjun Cha[2], Youjeong Yang[3], Seunghyun Choi[1], Yesol Woo[1], Jong-Won Lee[4], Docheon Ahn[5], Junhyuck Im[6], Yongjae Lee[6], Oc Hee Han[7,8,9], and Ji-Ho Yoon[1,3]

[1]Department of Energy and Resources Engineering, Korea Maritime and Ocean University, Busan, South Korea, [2]Department of Energy and Resources Engineering, Kangwon National University, Chuncheon, South Korea, [3]Department of Convergence Study on the Ocean Science and Technology, Ocean Science and Technology School, Korea Maritime and Ocean University, Busan, South Korea, [4]Department of Environmental Engineering, Kongju National University, Chungnam, South Korea, [5]Beamline Department, Pohang Accelerator Laboratory, Pohang, South Korea, [6]Department of Earth System Sciences, Yonsei University, Seoul, South Korea, [7]Western Seoul Center, Korea Basic Science Institute, Seoul, South Korea, [8]Graduate School of Analytical Science and Technology, Chungnam National University, Daejeon, South Korea, [9]Department of Chemistry and Nano-Science, College of Natural Sciences, Ewha Womans University, Seoul, South Korea

Abstract Understanding the stability of volatile species and their compounds under various surface and subsurface conditions is of great importance in gaining insights into the formation and evolution of planetary and satellite bodies. We report the experimental results of the temperature- and pressure-dependent structural transformation of methane hydrates in salt environments using in situ synchrotron X-ray powder diffraction, solid-state nuclear magnetic resonance, and Raman spectroscopy. We find that under pressurized and concentrated brine solutions methane hydrate forms a mixture of type I clathrate hydrate, ice, and hydrated salts. Under a low-pressure condition, however, the methane hydrates are decomposed through a rapid sublimation of water molecules from the surface of hydrate crystals, while NaCl · $2H_2O$ undergoes a phase transition into a crystal growth of NaCl via the migration of salt ions. In ambient pressure conditions, the methane hydrate is fully decomposed in brine solutions at temperatures above 252 K, the eutectic point of NaCl · $2H_2O$.

1. Introduction

Clathrate hydrates, which possess similar chemical properties to ice, can be stabilized using the van der Waals interaction between the small guest molecules (CH_4, CO_2, H_2, N_2, etc.) and the host water framework constructed by the hydrogen bonds in the water molecules [*Berecz and Bella-Achs*, 1983; *Sloan*, 2003; *Sloan and Koh*, 2008]. Several types of guest molecules are known to form the three common structures of clathrate hydrates, which are classified into structure I (sI), structure II (sII), and structure H (sH) hydrates [*Sloan*, 2003; *Sloan and Koh*, 2008]. In the icy matrix of clathrate hydrates, vast amounts of gas storage and selective guest enclathration from mixtures are possible, which has resulted in these hydrates garnering considerable attention in the energy and environmental fields over the past several decades [*Gudmundsson et al*., 1994; *Kang and Lee*, 2000; *Sun et al*., 2003; *Linga et al*., 2007; *Makogon et al*., 2007; *Park et al*., 2011; *Cha and Seol*, 2013; *Xu and Li*, 2014; *Seo et al*., 2015]. It has been proposed that clathrate hydrates could also exist on planetary or icy satellite bodies such as Mars [*Miller and Smythe*, 1970; *Pellenbarg et al*., 2003; *Thomas et al*., 2009], Titan [*Lunine and Stevenson*, 1987; *Loveday et al*., 2001; *Tobie et al*., 2006], and Enceladus [*Kieffer et al*., 2006; *Fortes*, 2007].

Chlorine salts, such as chlorides (Cl^-) and perchlorates (ClO_4^-), can provide a significant role in the liquid water stability [*Altheide et al*., 2009; *Chevrier et al*., 2009; *Hanley et al*., 2012]. Notably, the freezing point of water can be depressed to 204 K by chlorine salts owing to the alteration of the water chemical potential in brine solutions [*Chevrier et al*., 2009; *Hanley et al*., 2012]. The existence of chlorine salts on planetary or icy satellite bodies may support the existence of salty ocean, and thus, brine water is also believed to be present on the Martian surface in warm seasons [*McEwen et al*., 2011, 2014; *Ojha et al*., 2015]. The clathrate hydrates in the planetary and satellite bodies might be exposed to various thermodynamic conditions such as low-pressure and highly concentrated salt environments. For instance, a salty ocean containing clathrate hydrates is thought to exist within the subsurface of Enceladus because salt-rich ice particles, water vapor,

and volatile gases were detected within plumes emanating from Enceladus [*Postberg et al*., 2011]. Therefore, understanding the clathrate hydrate destabilization process in the salt environments on planetary and satellite bodies is important.

Based on this background, the following behaviors that occur in clathrate hydrates with salt environments are addressed: (1) the effect of salts on the crystal structure and guest distributions of the clathrate hydrates, (2) the clathrate hydrate dissociation in the presence of salts under various temperature and pressure conditions, and (3) the structural transition of the clathrate hydrates in salt environments during the hydrate decomposition. Methane hydrates were prepared in the presence of salts, and a suite of spectroscopic analyses combining X-ray diffraction (XRD), solid-state nuclear magnetic resonance (NMR), and Raman spectroscopy was performed in order to identify the crystal structure, guest distribution, and dissociation behavior of the methane hydrate samples. These results can provide useful insights into the structural transformation of the clathrate hydrates in salt environments.

2. Methods

2.1. Materials

Methane gas with a minimum purity of 99.99 mol % was obtained from Headong Gas Co. (South Korea). NaCl with a minimum purity of 99.5 mol % was supplied by Sigma-Aldrich. $MgCl_2$ with a minimum purity of 99.9 mol % was also supplied by Sigma-Aldrich. Deionized water was obtained using a purification unit.

2.2. Preparation of Methane Hydrates

A high-pressure cell with approximately 90 cm^3 of internal volume was initially charged with aqueous salt solutions and then pressurized with methane gas to the desired pressure condition. The high-pressure cell was maintained at 274 K and 10 MPa for at least 6 days, and the hydrate formation was monitored using the sudden pressure drops. After the complete hydrate conversion, the cell was immersed in liquid nitrogen, and the hydrate samples were ground with a 100 μm sieve under liquid nitrogen.

2.3. In Situ Synchrotron XRD

The XRD patterns of the methane hydrate samples were measured at 80 K using a synchrotron radiation with a step length of 0.01° and $\lambda = 1.5178$ Å at the Pohang Accelerator Laboratory (PAL). The phase identification was determined using the CheckCell software [*Laugier and Bochu*, 2000]. In situ temperature-dependent synchrotron XRD experiments were performed at the 9B high-resolution powder diffraction beamline ($\lambda = 1.4861$ Å) at PAL. Each diffraction pattern was scanned in the range of 5–125° with a step length of 0.04°. For the temperature-dependent XRD measurements, the sample temperature was varied from 100 to 250 K at intervals of 5 K. Changes in the phase fraction were derived from the Rietveld refinements using the General Structure Analysis System (GSAS) program [*Larson and Von Dreele*, 1994; *Toby*, 2001].

2.4. NMR Spectroscopy

Solid-state ^{13}C and ^{23}Na magic angle spinning (MAS) NMR spectra were acquired using a Bruker AVANCE II^+ 400 MHz spectrometer in a 9.4 T magnetic field using a 4 mm zirconia rotor. The ^{13}C MAS NMR spectra were obtained at 213 K and a Larmor frequency of 100.6 MHz under proton decoupling with a 7 kHz spinning rate, 30° pulse length of 1.6 μs, and 3 s pulse repetition delay time. The downfield-shifted carbon resonance peak of adamantane, which appeared at 38.56 ppm relative to tetramethylsilane, was used as an external chemical shift reference. The ^{23}Na MAS NMR spectra were acquired at a radio frequency of 105.84 MHz with a 7 kHz spinning rate, 30° pulse width of length of 1 μs, and 5 s pulse repetition delay time. An external chemical shift reference of 1 M NaCl aqueous solution was used.

2.5. Raman Spectroscopy

A maximum power of 150 mW from a 532 nm line of an Nd:YAG laser (Excelsior) source was used for the Raman spectroscopy. The laser spot size on the samples was approximately 20 μm, and a spectral resolution of approximately 1.5 cm^{-1} was provided from the combination of a spectrograph (SpectraPro) and a multichannel air-cooled CCD detector (Princeton Instruments). A Linkam temperature-controlled stage was used to control the system temperature during the Raman measurements with a stability of <0.1 K. For the temperature-dependent Raman measurements, the sample temperature on the microscope stage was varied from 130 to 270 K at intervals of 5 K.

3. Results and Discussion

First, methane hydrates in the presence of either of the two salts (4 wt % NaCl or $MgCl_2$) were prepared, and their crystal structures and characteristics were analyzed using XRD, solid-state ^{13}C MAS NMR, and Raman spectroscopy. Methane is known to be a sI hydrate former [*Sloan*, 2003; *Sloan and Koh*, 2008] with the occupation of methane molecules in both the small 5^{12} and large $5^{12}6^2$ cages, and the obtained XRD patterns indicate that there were no salt effects on the crystal structure of the methane hydrates in the presence of either of the two salts (4 wt % NaCl or $MgCl_2$) as depicted in Figure 1a. The crystal structures of both methane hydrate samples in the presence of 4 wt % NaCl or $MgCl_2$ were identified as cubic unit cell structures with a space group of *Pm3n* and a lattice parameter of $a = 11.8862$ Å for the NaCl salt system and $a = 11.8824$ Å for the $MgCl_2$ salt system. These crystal structures with the lattice parameters are in good agreement with the literature [*Sloan*, 2003; *Sloan and Koh*, 2008]. Hexagonal ice (Ih) phases were also observed in the XRD patterns (Figure 1a). Figures 1b and 1c show the solid-state ^{13}C MAS NMR and Raman spectra of methane clathrate hydrate samples with and without 4 wt % NaCl. Raman spectroscopy was used to determine the crystal structure and cage occupancy of the methane hydrates with and without 4 wt % NaCl (Figure 1c). For both methane hydrate samples with and without 4 wt % NaCl, the Raman bands corresponding to the C–H vibration of the methane molecules in the large $5^{12}6^2$ and small 5^{12} cages of the sI hydrate were also observed at 2905 and 2915 cm^{-1}, respectively [*Sum et al*., 1997; *Subramanian et al*., 2000]. There were no changes in the spectral position of the Raman bands and their peak area ratio (A_L/A_S). Therefore, these results indicate that there were no changes in the cage occupancy and crystal structure of the methane hydrates formed in brine solutions. Similar trends could be also observed in the solid-state ^{13}C NMR spectra as depicted in Figure 1b. It is known that the ^{13}C resonance peaks at −4.2 and −6.6 ppm can be assigned to methane molecules trapped in the small and large cages of sI hydrates, respectively [*Sloan and Koh*, 2008]. The ^{13}C resonance peak at −11.0 ppm can be attributed to the release of the methane gas due to the partial decomposition of the methane hydrates. Using the area ratios of the NMR peaks at −4.2 and −6.6 ppm, the fractional occupancy ratio (θ_L/θ_S) of methane in the large and small cages of the sI hydrate can be evaluated to be $\theta_L/\theta_S = \sim 1.07$ ($= A_L/3A_S$) for both methane hydrates with and without the 4 wt % NaCl. Differences were not found in the ^{13}C resonance peak position and fractional occupancy ratio of the methane molecules in the hydrate cages; thus, these are consistent with the Raman results.

We conclude that the salt ions do not affect the crystal structure and guest distribution of the methane hydrates during the hydrate formation, and we also confirm that the salts are concentrated in brine solutions during the methane hydrate formation, resulting to the formation of hydrohalite after the hydrate formation as shown in Figures 1a and 1c. From the XRD patterns, the hydrated salt compounds representing $NaCl \cdot 2H_2O$ and $MgCl_2 \cdot 12H_2O$ were observed, which result from the phase behavior of the water-salt binary systems (Figure S1 in the supporting information), and the Bragg signals from the hydrated salt compounds are indexed at the bottom of Figure 1a. In Figure 1c, the Raman spectra (red lines) from the methane hydrate sample with 4 wt % NaCl exhibited Raman bands of hydrohalite (hydrated salt, $NaCl \cdot 2H_2O$) at approximately 3405, 3423, and 3540 cm^{-1} [*Bakker*, 2004; *Wise et al*., 2012]. In addition, it should be noted that the O–H stretching vibration of the water molecules in the hydrogen-bonded frameworks of the sI hydrate exhibited a blue shift (approximately 6 cm^{-1}) with the addition of the 4 wt % NaCl salts as depicted in Figure 1c. Several researchers have investigated the contribution of hydrogen-bonded water molecules to the Raman signals from the O–H stretching vibration regions [*Smith et al*., 2005; *Đuričković et al*., 2010], and they concluded that the strongly coupled hydrogen-bonding interaction in the water molecules induced the left shoulder of the Raman signals from the O–H stretching vibration region, whereas the right shoulder of the Raman signals from the O–H stretching vibration region might result from the weakly coupled hydrogen-bonding interaction in the water molecules [*Smith et al*., 2005; *Đuričković et al*., 2010]. Therefore, we propose that the water-water interaction in the hydrogen-bonded framework of the sI hydrate is affected by the ion-water interaction between the water and salt ions in the brine solutions on the surface of the methane hydrate crystals.

Methane hydrate in icy planetary bodies might be exposed to various thermodynamic conditions such as low-pressure and highly concentrated salt environments, which lead to a phase transition. In this case, it can be expected that the decomposition behavior of the methane hydrate under these conditions differs significantly from the self-preservation phenomena at an ambient pressure, which is typically observed for

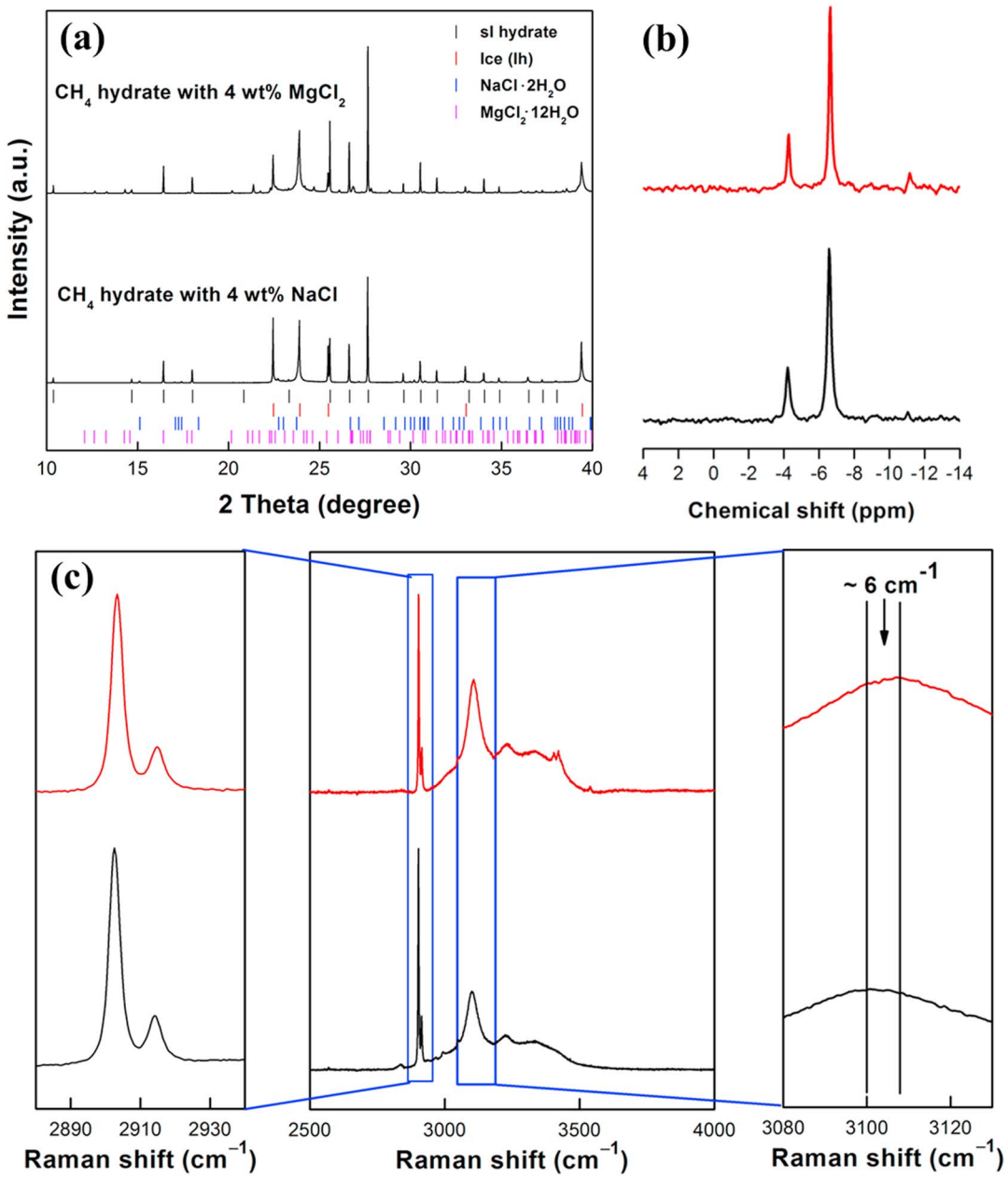

Figure 1. (a) XRD patterns of methane clathrate hydrates formed in aqueous salt solutions. XRD measurements were performed at 80 K and 10^{-7} torr. (b) Solid-state ^{13}C MAS NMR spectra of pure methane clathrate hydrate (black line) and methane clathrate hydrate formed with 4 wt % NaCl (red line). NMR measurements were performed at 213 K and ambient pressure. (c) Raman spectra of pure methane clathrate hydrate (black lines) and methane clathrate hydrate formed with 4 wt % NaCl (red lines). Raman measurements were performed at 120 K and ambient pressure.

methane hydrates. In addition, the presence of salt with hydrate phase in icy planetary bodies may provide significant effects on the hydrate decomposition, and thus, a key question arises as to the role of the salts in the hydrate phase during the hydrate decomposition. In order to elucidate the phase transition of the methane hydrates under planetary environments and the role of salts in the hydrate phase during the hydrate decomposition, in situ synchrotron XRD measurements were performed in the temperature range of 100–250 K using the methane hydrate formed in the aqueous NaCl solutions (Figure 2). For temperature-dependent XRD measurements, the methane hydrate formed in the 4 wt % NaCl solution

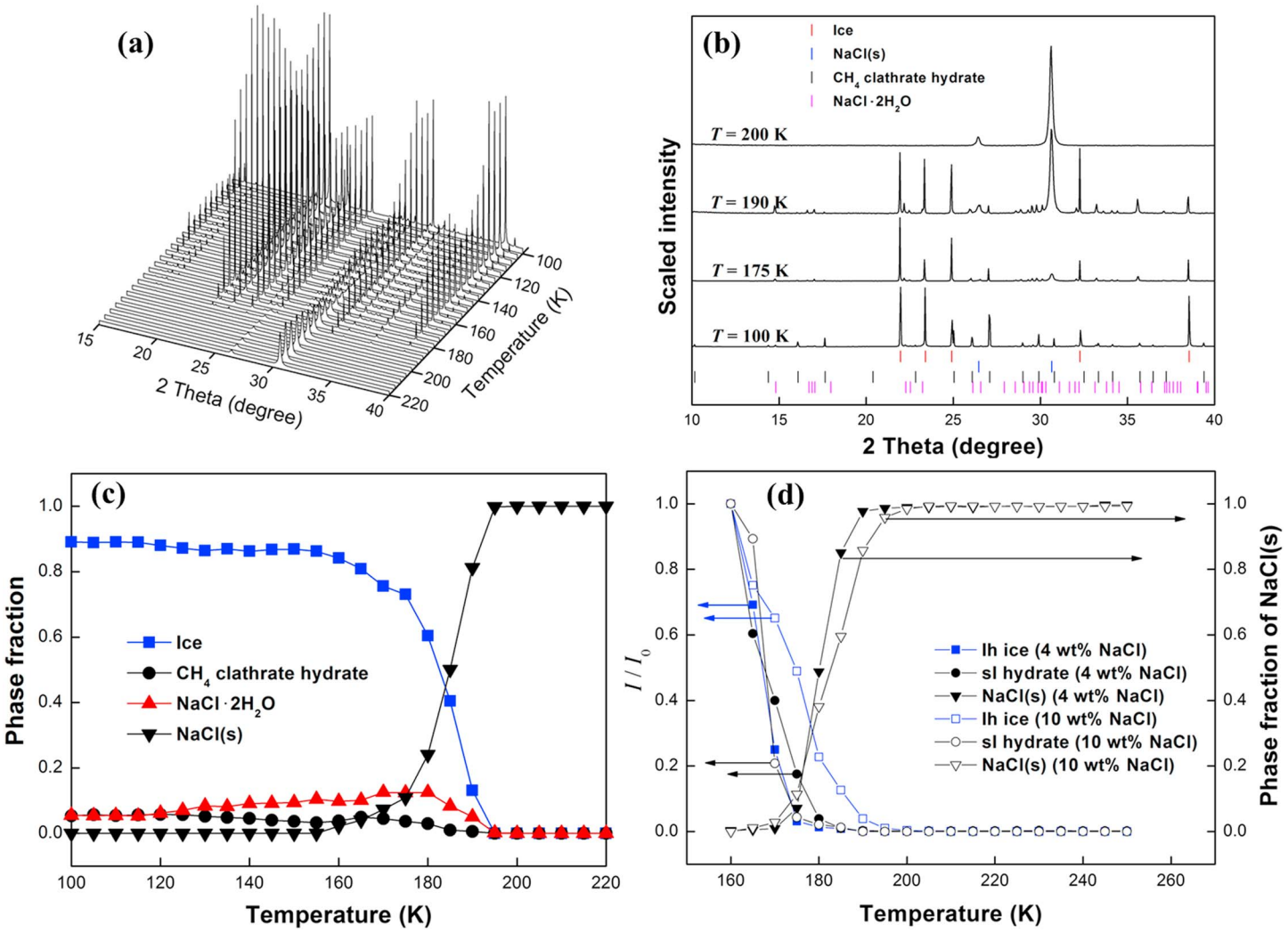

Figure 2. (a) In situ temperature-dependent synchrotron XRD patterns of methane clathrate hydrates formed with 4 wt % NaCl. (b) Selected XRD patterns taken from Figure 2a. (c) Phase fraction of methane clathrate hydrate, ice, NaCl · $2H_2O$, and NaCl(s) in methane clathrate hydrate formed with 4 wt % NaCl as a function of temperature, derived from the Rietveld refinements. (d) Normalized XRD intensity and phase fraction of methane clathrate hydrate, ice, and NaCl(s) as a function of temperature and salt concentration. All measurements were performed at 10^{-7} torr.

sample was tested in the range of 5–125° with a step length of 0.04° from 100 to 220 K at intervals of 5 K. Figures 2a and 2b present enlarged XRD patterns of the methane hydrates formed in the 4 wt % NaCl solution between 15° and 40°, and the phase transition of the ice, methane clathrate hydrate, and salts can be seen as the temperature increases. The Rietveld refinements using the GSAS program [*Larson and Von Dreele*, 1994; *Toby*, 2001] were performed in order to identify the phase fraction of the ice, methane clathrate hydrate, and salts in the methane hydrate formed in the 4 wt % NaCl solution sample (Figure 2c). In this measurement, the depleted planetary atmospheric conditions, which lower the pressure of the synchrotron XRD sample chamber to approximately 10^{-7} torr, are demonstrated. Therefore, the phase fractions of the initial solid mixture at 100 K and approximately 10^{-7} torr were found to be 0.88 for the ice phase, 0.06 for the methane clathrate hydrate phase, and 0.06 for the NaCl · $2H_2O$ solid phase. Previously, *Falabella* [1975] reported the three-phase (ice-hydrate-vapor) equilibrium conditions of methane hydrates at temperatures below 273 K. It should be noted that the equilibrium dissociation pressure of the methane hydrate at 148.8 K is estimated to be 5.3 kPa (approximately 40 torr). Therefore, it can be expected that the methane hydrates are thermodynamically unstable at 100–160 K and approximately 10^{-7} torr; thus, they

are preserved by the sheets of ice and/or the hydrated salt $NaCl \cdot 2H_2O$. In particular, the amount of methane clathrate hydrates was nearly intact in the temperature range of 100–160 K as seen in Figure 2c although the pure methane clathrate hydrate was thermodynamically unstable at a pressure of approximately 10^{-7} torr [*Falabella*, 1975]. *Bryson et al*. [1974] investigated the sublimation rates and vapor pressures of H_2O in the temperature range of 131–188 K, and the results demonstrated that the vapor pressures of H_2O at 131.8 K and 148.5 K were 6.33×10^{-10} and 4.70×10^{-8} torr, respectively. Upon increasing the temperature to 175 K, the vapor pressure of the H_2O increased significantly and resulted in 1.49×10^{-5} torr at 174.6 K. Therefore, an abrupt change in the phase fraction near 160 K (Figure 2c) is closely related to the vapor pressure of the H_2O. In the temperature range of 100 to 160 K, the solid phases of ice and $NaCl \cdot 2H_2O$ exposed to the pressure of approximately 10^{-7} torr were thermodynamically stable and contributed to the strong preservation of the methane hydrate. However, upon increasing the temperature to >160 K, the ice phase and hydrated salt compounds began to have rapid sublimation; thus, a new set of diffraction peaks began to grow (Figure 2b), which signaled the phase transition of $NaCl \cdot 2H_2O$ to crystalline NaCl solids. With a further increase in the temperature, the amount of crystalline NaCl solids increased, as depicted in Figure 2c.

In order to clearly observe the formation of the crystalline NaCl solids during the hydrate decomposition, in situ synchrotron XRD measurements were tested in the temperature range of 160–250 K using the methane hydrate formed in the 4 wt % NaCl solution and 10 wt % NaCl solution samples. Figures S2 and S3 in the supporting information present the enlarged XRD patterns of the methane hydrates formed in the 4 wt % and 10 wt % NaCl aqueous solutions between 15° and 40°. The normalized XRD intensity of the methane clathrate hydrate and ice and the phase fraction of NaCl(s) as a function of the temperature and salt concentration are depicted in Figure 2d. Due to the sublimation of H_2O above 160 K, the relative XRD intensity of the sI hydrate and hexagonal ice phases rapidly decreased as the temperature increased, whereas the phase fraction of the crystalline NaCl solids increased for both methane hydrates formed in the 4 wt % and 10 wt % NaCl aqueous solutions. This is a clear demonstration that the rapid sublimation of H_2O from the surface of the ice, methane clathrate hydrate, and $NaCl \cdot 2H_2O$ accelerated the phase transition to crystalline NaCl solids in low-pressure conditions (~10^{-7} torr). In addition, the shape of the diffraction peaks for the crystalline NaCl solids began broader than those of the ice and $NaCl \cdot 2H_2O$. This is suspected to result from a crystal growth effect of the crystalline NaCl solids via the migration of salt ions. At temperatures above 200 K, the XRD patterns clearly indicated that only crystalline NaCl solids existed, as seen in Figures 2c and 2d.

The decomposition behavior of the methane clathrate hydrates that formed in the 0, 4, and 10 wt % NaCl solutions was also investigated at an ambient pressure using Raman spectroscopy in the temperature range of 130–270 K as depicted in Figures 3a, 3b, and S4 in the supporting information. The Raman bands at 2905 cm^{-1} corresponding to the methane molecules in the large $5^{12}6^2$ cages of the sI clathrate hydrates were normalized using the Raman band at 3150 cm^{-1}, which represents the O–H stretching vibration of the water molecules; then, their relative intensities were proposed as a function of the temperature (Figure 3c). Similar to the decomposition behavior in low-pressure conditions (pressure = approximately 10^{-7} torr), the amount of methane clathrate hydrates remained nearly intact in the temperature range of 100–160 K; however, the methane clathrate hydrates in ambient pressure exhibited a significant self-preservation effect in the temperature range of 160–250 K. In particular, it appeared that the suppressed decomposition behavior of the methane clathrate hydrates with brine solutions was very similar to that of the pure methane clathrate hydrates (Figure 3c). However, at temperatures above 255 K, the Raman spectra of the methane hydrates formed in the brine solutions disappeared (Figure S5 in the supporting information), which indicates the full decomposition of the methane hydrates formed in the NaCl solutions.

In order to identify the true role of salts during the hydrate decomposition, solid-state ^{23}Na MAS NMR measurements were performed in the temperature range of 213–253 K for the methane clathrate hydrates that formed in 4 wt % NaCl brine solutions (Figure 3d). A broad NMR signal was observed at 3.6 ppm, which indicates the ^{23}Na resonance peak of $NaCl \cdot 2H_2O$ at temperatures of 213 K and 233 K [*Cho et al*., 2002]. Upon increasing the temperature to 253 K, the broad NMR peak disappeared, whereas a new sharp peak was observed at 0.8 ppm, which represents the ^{23}Na resonance peak of the Na^+ in the aqueous salt solution [*Cho et al*., 2002]. In particular, the eutectic transition in the NaCl–H_2O binary system occurred at approximately 252 K, where the $NaCl \cdot 2H_2O$ melted in equilibrium with the ice and liquid [*Linke*, 1965; *Marion and Farren*, 1999; *Koop et al*., 2000]. Therefore, the combination of the Raman and solid-state NMR

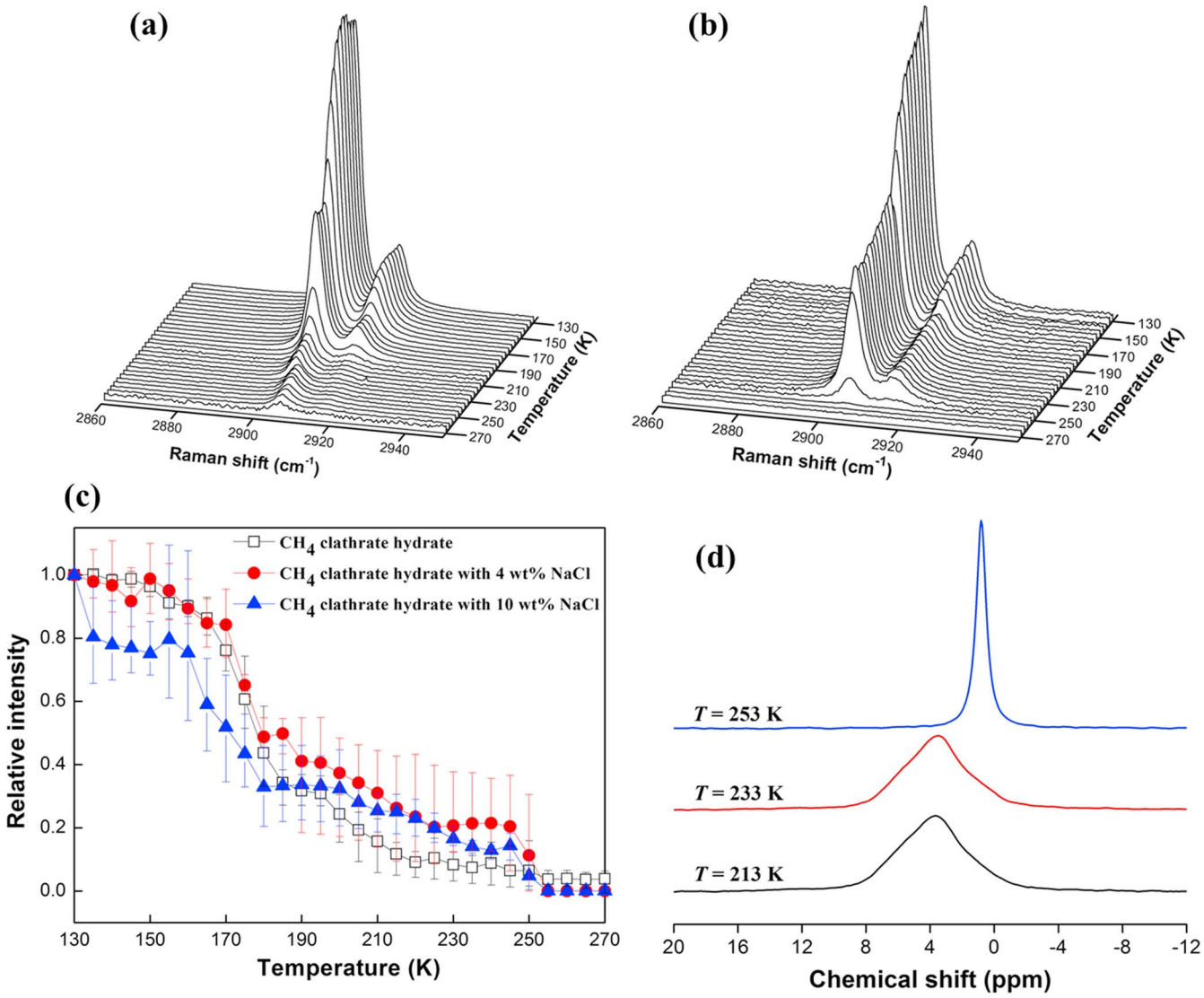

Figure 3. Temperature-dependent Raman spectra of methane molecules trapped in (a) pure methane clathrate hydrate and (b) methane clathrate hydrate formed with 4 wt % NaCl. (c) Normalized Raman intensity of methane molecules trapped in methane clathrate hydrate formed with and without salts. (d) Solid-state ^{23}Na MAS NMR spectra of methane clathrate hydrate formed with 4 wt % NaCl. All Raman and NMR measurements were performed at ambient pressure.

spectroscopy indicates that the significant phase transition of $NaCl \cdot 2H_2O$ occurred at the eutectic point (approximately 252 K), and thus, methane clathrate hydrates are fully decomposed in brine solutions at temperatures above 252 K. However, at temperatures below 252 K, the existence of $NaCl \cdot 2H_2O$ induced a negligible effect on the clathrate hydrate destabilization regardless of the salt concentration. These results provide useful insights into the phase transition of clathrate hydrates in salt environments, particularly under low-temperature and low-pressure conditions, which are similar to planetary environments, and might be important for a better understanding of hydrate decomposition via salt migration.

4. Conclusion and Implications

The experimental results of the temperature- and pressure-dependent structural transformation and salt migration of methane hydrates in salt environments were presented. The crystal structures and guest distribution of the clathrate hydrates with and without salts were analyzed using the spectroscopic tools of XRD,

Raman, and solid-state NMR spectroscopy. The methane hydrate that formed in the NaCl aqueous solution exhibited slight changes in the hydrogen-bonded interaction between water molecules, even though the addition of NaCl during the hydrate formation cannot affect the crystal structure and guest distribution of the methane hydrate. Under low-pressure conditions, the methane hydrates in the salt environments decomposed through rapid sublimation of the H_2O from the surfaces of the ice, methane clathrate hydrates, and $NaCl \cdot 2H_2O$, which led to the crystal growth of crystalline NaCl solids via migration of the salt ions. In ambient pressure conditions, the existence of $NaCl \cdot 2H_2O$ induced a negligible effect on the clathrate hydrate destabilization regardless of the salt concentration. However, the methane clathrate hydrates were fully decomposed in the brine solutions at temperatures above the eutectic point of $NaCl \cdot 2H_2O$.

The presence of methane and carbon dioxide clathrate hydrates within the Martian subsurface may be of critical importance in understanding the geomorphic evolution of Mars. Recent findings also support the hypothesis that hydrated salts and liquid water coexist on the surface of Mars [*Ojha et al*., 2015; *McEwen et al*., 2014]. Considering seasonal temperature changes on Mars, the stability of clathrate hydrates may be influenced by the hydrated salts and/or brines penetrated into the Martian subsurface. In addition to this Martian clathrate hydrate scenario, a similar hypothesis might be proposed for the plume of Enceladus [*Kieffer et al*., 2006; *Fortes*, 2007]. Given that the plume consists of water vapor, salty-ice grains, and insoluble gases such as CH_4, CO_2, and N_2, Enceladus is likely to have a salty subsurface ocean beneath its frozen surface in the south pole where clathrate hydrates are formed and drive the plume [*Postberg et al*., 2009, 2011]. We also know that the temperature in the south polar fracture regions "tiger stripes" is higher (110–180 K) than the mean surface temperature (80–90 K) [*Kieffer et al*., 2006; *Spencer et al*., 2006; *Showman et al*., 2013; *Behounková et al*., 2013]. Therefore, the plume composition through Enceladus' cryovolcanism may undergo variations depending on the regional changes in temperature and pressure. The in situ synchrotron XRD experiments presented in this study would give good estimates in the phase transition of clathrate hydrates in salt environments, especially under low-temperature and low-pressure conditions, similar to these planetary environments.

Acknowledgments
This research was supported by the Midcareer Research Program (2015003772) through a National Research Foundation of Korea (NRF) grant founded by the Ministry of Science, ICT, and Future Planning. The solid-state NMR data were acquired at the Western Seoul Center of KBSI, and synchrotron XRD measurements were performed at PAL in POSTECH. The authors acknowledge Sun Ha Kim for performing the NMR experiments. Donghoon Shin and Minjun Cha contributed equally to this work.

References

Altheide, T., V. Chevrier, C. Nicholson, and J. Denson (2009), Experimental investigation of the stability and evaporation of sulfate and chloride brines on Mars, *Earth Planet. Sci. Lett.*, *282*, 69–78, doi:10.1016/j.epsl.2009.03.002.

Bakker, R. J. (2004), Raman spectra of fluid and crystal mixtures in the systems H_2O, H_2O-NaCl and H_2O-$MgCl_2$ at low temperatures: Applications to fluid-inclusion research, *Can. Mineral.*, *42*, 1283–1314, doi:10.2113/gscanmin.42.5.1283.

Behounková, M., G. Tobie, G. Choblet, and O. Čadek (2013), Impact of tidal heating on the onset of convection in Enceladus's ice shell, *Icarus*, *226*, 898–904, doi:10.1016/j.icarus.2013.06.033.

Berecz, E., and M. Bella-Achs (1983), *Gas Hydrates (Studies in Inorganic Chemistry)*, Elsevier, Amsterdam.

Bryson, C. E., V. Cazcarra, and L. L. Levenson (1974), Sublimation rates and vapor pressures of H_2O, CO_2, N_2O, and Xe, *J. Chem. Eng. Data*, *19*, 107–110, doi:10.1021/je60061a021.

Cha, J. H., and Y. Seol (2013), Increasing gas hydrate formation temperature for desalination of high salinity produced water with secondary guests, *Sustainable Chem. Eng.*, *1*, 1218–1224, doi:10.1021/sc400160u.

Chevrier, V. F., J. Hanley, and T. S. Altheide (2009), Stability of perchlorate hydrates and their liquid solutions at the Phoenix landing site, Mars, *Geophys. Res. Lett.*, *36*, L10202, doi:10.1029/2009GL037497.

Cho, H., P. B. Shepson, L. A. Barrie, J. P. Cowin, and R. Zaveri (2002), NMR investigation of the quasi-brine layer in ice/brine mixtures, *J. Phys. Chem. B*, *106*, 11,226–11,232, doi:10.1021/jp020449+.

Đuričković, I., M. Marchetti, R. Claverie, P. Bourson, J. Chassot, and M. D. Fontana (2010), Experimental study of NaCl aqueous solutions by Raman spectroscopy: Towards a new optical sensor, *Appl. Spectrosc.*, *64*, 853–857.

Falabella, B. J. (1975), A study of natural gas hydrates, PhD thesis, Univ. of Mass., Univ. of Microfilms No. 76-5849, Ann Arbon, Mich.

Fortes, A. D. (2007), Metasomatic clathrate xenoliths as a possible source for the south polar plumes of Enceladus, *Icarus*, *191*, 743–748, doi:10.1016/j.icarus.2007.06.013.

Gudmundsson, J. S., M. Parlaktuna, and A. A. Khokhar (1994), Storage natural gas as frozen hydrate, *SPE Prod. Facilities*, *9*, 69–73, doi:10.2118/24924-PA.

Hanley, J., V. F. Chevrier, D. J. Berget, and R. D. Adams (2012), Chlorate salts and solutions on Mars, *Geophys. Res. Lett.*, *39*, L08201, doi:10.1029/2012GL051239.

Kang, S. P., and H. Lee (2000), Recovery of CO_2 from flue gas using gas hydrate: Thermodynamic verification through phase equilibrium measurements, *Environ. Sci. Technol.*, *34*, 4397–4400, doi:10.1021/es001148l.

Kieffer, S. W., X. Lu, C. M. Bethke, J. R. Spencer, S. Marshak, and A. Navrotsky (2006), A clathrate reservoir hypothesis for Enceladus' south polar plume, *Science*, *314*, 1764–1766, doi:10.1126/science.1133519.

Koop, T., A. Kapilashrami, L. T. Molina, and M. J. Molina (2000), Phase transitions of sea-salt/water mixtures at low temperatures: Implications for ozone chemistry in the polar marine boundary layer, *J. Geophys. Res.*, *105*, 26,393–26,402, doi:10.1029/2000JD900413.

Larson, A. C., and R. B. Von Dreele (1994), General Structure Analysis System (GSAS), Los Alamos National Laboratory Report LAUR 86-748.

Laugier, J., and B. Bochu (2000), Laboratoire des Materiaus et du Genie Physique, Ecole Superieure de Physique de Grenble. [Available at http://www.ccp14.ac.uk.]

Linga, P., R. Kumar, and P. Englezos (2007), The clathrate hydrate process for post and pre-combustion capture of carbon dioxide, *J. Hazard. Mater.*, *149*, 625–629, doi:10.1016/j.jhazmat.2007.06.086.

Linke, W. F. (1965), *Solubilities of Inorganic and Metal Organic Compounds*, Am. Chem. Soc., Washington, D. C.

Loveday, J. S., R. J. Nelmes, M. Guthrie, S. A. Belmonte, D. R. Allan, D. D. Klug, J. S. Tse, and Y. P. Handa (2001), Stable methane hydrate above 2 GPa and the source of Titan's atmospheric methane, *Nature*, *410*, 661–663, doi:10.1038/35070513.

Lunine, J. I., and D. J. Stevenson (1987), Clathrate and ammonia hydrates at high pressure: Application to the origin of methane on Titan, *Icarus*, *70*, 61–77, doi:10.1016/0019-1035(87)90075-3.

Makogon, Y. F., S. A. Holditch, and T. Y. Makogon (2007), Natural gas-hydrates—A potential energy source for the 21st century, *J. Petrol. Sci. Eng.*, *56*, 14–31, doi:10.1016/j.petrol.2005.10.009.

Marion, G. M., and R. F. Farren (1999), Mineral solubilities in the Na-K-Mg-Ca-Cl-SO_4-H_2O system: A re-evaluation of the sulfate chemistry in the Spencer-Moller-Weare model, *Geochim. Cosmochim. Acta*, *63*, 1305–1318, doi:10.1016/S0016-7037(99)00102-7.

McEwen, A. S., L. Ojha, C. M. Dundas, S. S. Mattson, S. Byrne, J. J. Wray, S. C. Cull, S. L. Murchie, N. Thomas, and V. C. Gulick (2011), Seasonal flows on warm Martian slopes, *Science*, *333*, 740–743, doi:10.1126/science.1204816.

McEwen, A. S., C. M. Dundas, S. S. Mattson, A. D. Toigo, L. Ojha, J. J. Wray, M. Chojnacki, S. Byrne, S. L. Murchie, and N. Thomas (2014), Recurring slope lineae in equatorial regions of Mars, *Nat. Geosci.*, *7*, 53–58, doi:10.1038/ngeo2014.

Miller, S. L., and W. D. Smythe (1970), Carbon dioxide clathrate in the Martian ice cap, *Science*, *170*, 531–533, doi:10.1126/science.170.3957.531.

Ojha, L., M. B. Wilhelm, S. L. Murchie, A. S. McEwen, J. J. Wray, J. Hanley, M. Massé, and M. Chojnacki (2015), Spectral evidence for hydrated salts in recurring slope line on Mars, *Nat. Geosci.*, *8*, 829–832, doi:10.1038/ngeo2546.

Park, K. N., S. Y. Hong, J. W. Lee, and J. D. Lee (2011), A new apparatus for seawater desalination by gas hydrate process and removal characteristics of dissolved minerals (Na^+, Mg^{2+}, Ca^{2+}, K^+, B^{3+}), *Desalination*, *274*, 91–96, doi:10.1016/j.desal.2011.01.084.

Pellenbarg, R. E., M. D. Max, and S. M. Clifford (2003), Methane and carbon dioxide hydrates on Mars: Potential origins, distribution, detection, and implications for future in situ resource utilization, *J. Geophys. Res.*, *108*, 8042–8047, doi:10.1029/2002JE001901.

Postberg, F., S. Kempf, J. Schmidt, N. Brilliantov, A. Beinsen, B. Abel, U. Buck, and R. Srama (2009), Sodium salts in E-ring ice grains from an ocean below the surface of Enceladus, *Nature*, *459*, 1098–1101, doi:10.1038/nature08046.

Postberg, F., J. Schmidt, J. Hillier, S. Kempf, and R. Srama (2011), A salt-water reservoir as the source of a compositionally stratified plume on Enceladus, *Nature*, *474*, 620–622, doi:10.1038/nature10175.

Seo, Y., D. Moon, C. Lee, J. Park, B. Kim, G. Lee, P. Dotel, J.-W. Lee, M. Cha, and J.-H. Yoon (2015), Equilibrium, kinetics, and spectroscopic studies of SF_6 hydrate in NaCl electrolyte solution, *Environ. Sci. Technol.*, *49*, 6045–6050, doi:10.1021/acs.est.5b00866.

Showman, A. P., L. Han, and W. B. Hubbard (2013), The effect of an asymmetric core on convection in Enceladus' ice shell: Implications for south polar tectonics and heat flux, *Geophys. Res. Lett.*, *40*, 5610–5614, doi:10.1002/2013GL057149.

Sloan, E. D. (2003), Fundamental principles and applications of natural gas hydrates, *Nature*, *426*, 353–359, doi:10.1038/nature02135.

Sloan, E. D., and C. A. Koh (2008), *Clathrate Hydrates of Natural Gases*, 3rd ed., CRC Press, Boca Raton, Fla.

Smith, J. D., C. D. Cappa, K. R. Wilson, R. C. Cohen, P. L. Geissler, and R. J. Saykally (2005), Unified description of temperature-dependent hydrogen-bond rearrangements in liquid water, *Proc. Natl. Acad. Sci. U.S.A.*, *102*, 14,171–14,174, doi:10.1073/pnas.0506899102.

Spencer, J. R., J. C. Pearl, M. Segura, A. Mamoutkine, P. Romani, B. J. Buratti, A. R. Hendrix, L. J. Spilker, and R. M. C. Lopes (2006), Cassini encounters Enceladus: Background and the discovery of a south polar hot spot, *Science*, *311*, 1401–1405, doi:10.1126/science.1121661.

Subramanian, S., R. A. Kini, S. F. Dec, and E. D. Sloan (2000), Structural transition studies in methane + ethane hydrates using Raman and NMR, *Ann. NY Acad. Sci.*, *912*, 873–886, doi:10.1111/j.1749-6632.2000.tb06841.x.

Sum, A. K., R. C. Burruss, and E. D. Sloan (1997), Measurements of clathrate hydrates via Raman spectroscopy, *J. Phys. Chem. B*, *101*, 7371–7377, doi:10.1021/jp970768e.

Sun, Z., R. Wang, R. Ma, K. Guo, and S. Fan (2003), Natural gas storage in hydrate with the presence of promoters, *Energy Convers. Manage.*, *44*, 2733–2742, doi:10.1016/S0196-8904(03)00048-7.

Thomas, C., O. Mousis, S. Picaud, and V. Ballenegger (2009), Variability of the methane trapping in Martian subsurface clathrate hydrates, *Planet. Space Sci.*, *57*, 42–47, doi:10.1016/j.pss.2008.10.003.

Tobie, G., J. I. Lunine, and C. Sotin (2006), Episodic outgassing as the origin of atmospheric methane on Titan, *Nature*, *440*, 61–64, doi:10.1038/nature04497.

Toby, B. H. (2001), EXPGUI, a graphical user interface for GSAS, *J. Appl. Crystallogr.*, *34*, 210–213, doi:10.1107/S0021889801002242.

Wise, M. E., K. J. Baustian, T. Koop, M. A. Freedom, E. J. Jensen, and M. A. Tolbert (2012), Depositional ice nucleation onto crystalline hydrated NaCl particles: A new mechanism for ice formation in the troposphere, *Atmos. Chem. Phys.*, *12*, 1121–1134, doi:10.5194/acp-12-1121-2012.

Xu, C.-G., and X.-S. Li (2014), Research progress of hydrate-based CO_2 separation and capture from gas mixtures, *RSC Adv.*, *4*, 18,301–18,316, doi:10.1039/C4RA00611A.